Job: Dopico
Chapter: 15_Dimova
Template: MIMB/7x10/Temp/01.02.07

Operator: IBH
Date: 17/05/07
Revision: 1st Revises

15

Optical Dynamometry to Study Phase Transitions in Lipid Membranes

R. Dimova and B. Pouligny

Summary

The fluidity of the lipid matrix of cell membranes is crucial for the mobility of various inclusions like proteins. When the lipid bilayer undergoes phase transition from fluid-to-gel phase, the shear surface viscosity of the membrane diverges, thus hindering the motion of the membrane inclusions. On the other hand, the membrane bending stiffness drops down, and below the main phase transition, drastically increases with lowering the temperature. A tool to study the membrane properties when the lipid bilayer crosses the phase transition is provided by optical trapping and manipulation of microspheres attached to the membrane. Giant unilamellar vesicles are used, which allow for direct visualization of the membrane response, as model membranes. Following the motion of one or two particles attached to a vesicle, the microscope can provide evidence for the membrane elasticity and state of fluidity. As forces acting on the spheres, one can use gravity, thermal noise, or radiation pressure force.

Key Words: Bending stiffness; giant vesicles; model membranes; optical trapping; phase transition; shear surface viscosity.

1. Introduction

Optical trapping has been extensively exploited for biophysical applications, especially in recent years, when single molecule manipulation has become of intense interest. The great advantage of the technique of optical trapping consists of the possibility to manipulate objects without having to establish a direct mechanical contact with them. Instead, the momentum of light from a laser comes into play to form tiny tweezers for handling microscopic objects. Nowadays, two main versions of optical trapping are broadly used. One is the conventional (also commercially available), single-beam tweezers formed by focusing a laser beam in a sample through a high numerical aperture objective. The latter limits the studies with such a setup to short working distances. This version of the optical trap is currently applied to trapping of particles up to a few microns in diameter. The second version (which, as a matter of fact, was historically first) (*see* **ref. *1***) is based on two counter-propagating beams focused by two long-focal-distance objectives. From the viewpoint of optical architecture and tuning, the single-beam trap is simple; whereas the double-beam trap is more complex. However the latter offers the advantage of a much larger working distance, and is better suited to manipulation of large (several micrometers) objects and structures. In addition, because the beams are only weakly focused, optical damage (essentially heating) is in general weak. Basically, the choice of one or the other type of optical tweezers depends on the application and the studied system. This chapter reports on experiments involving large particles (up to 10 μm in radius) inside a thick chamber, for which

From: *Methods in Molecular Biology, vol. 400: Methods in Membrane Lipids*
Edited by: A. M. Dopico © Humana Press Inc., Totowa, NJ

Job: Dopico
Chapter: 15_Dimova
Template: MIMB/7x10/Temp/01.02.07

Operator: IBH
Date: 17/05/07
Revision: 1st Revises

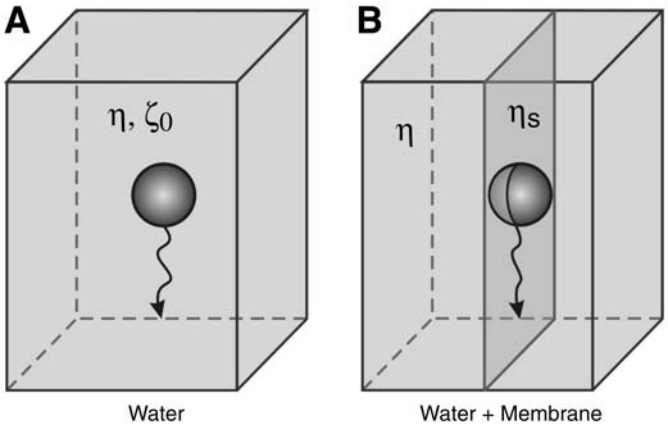

Fig. 1. **(A)** When a particle moves freely in bulk solution of viscosity η the drag coefficient (ζ_0) is given by the Stokes friction. **(B)** A particle attached to a membrane of shear surface viscosity η_S experiences an additional friction resulting in $\zeta = \zeta_0 + \zeta_m$.

the double-beam version of optical trapping was most appropriate. The setup is described in details elsewhere ***(2)*** (*see* also **ref. *3*** for additional characteristics).

Latex particles of size between 1 and 20 μm were used to explore the mechanical and rheological properties of model lipid membranes. These were in the form of giant vesicles ***(4)***, which are closed sacs made of a lipid bilayer in a water environment. Their relatively large size (several tens of micrometers), compared with conventional vesicles (few hundreds of nanometer in size), allows for direct microscopy observation.

1.1. Shear Surface Viscosity Measurements

When a latex microsphere is attached to a membrane, it can be used as a probe of the membrane state (*see* **Fig. 1**). In spite of the fact that the particle is several orders of magnitude larger than the lipid membrane (~5 nm in thickness), the particle motion can be affected by the displacement of the surrounding lipids. Motion of the lipids and of the water that is confined inside the vesicle increase the particle hydrodynamic drag coefficient (ζ). When the vesicle is much larger than the particle, ζ can be approximately decomposed according to:

$$\zeta = \zeta_0 + \zeta_m \tag{1}$$

where ζ_0 is the background or Stokes friction of the particle in the bulk solution, $\zeta_0 = 6\pi\eta a$, and ζ_m is the excess friction because of shearing the membrane. η is the viscosity of the surrounding fluid (the water solution), and *a* is the particle radius. The problem of a sphere straddling a membrane has already been theoretically treated in detail ***(5,6)*** and the results experimentally applied ***(7)***. The membrane contribution to the friction coefficient was found to depend almost linearly on the membrane shear surface viscosity (η_S) and only weakly on the particle radius:

$$\zeta_m \cong 2.93\eta_S \left(\frac{\eta a}{\eta_S}\right)^{0.1} \tag{2}$$

Job: Dopico
Chapter: 15_Dimova
Template: MIMB/7x10/Temp/01.02.07

Operator: IBH
Date: 17/05/07
Revision: 1st Revises

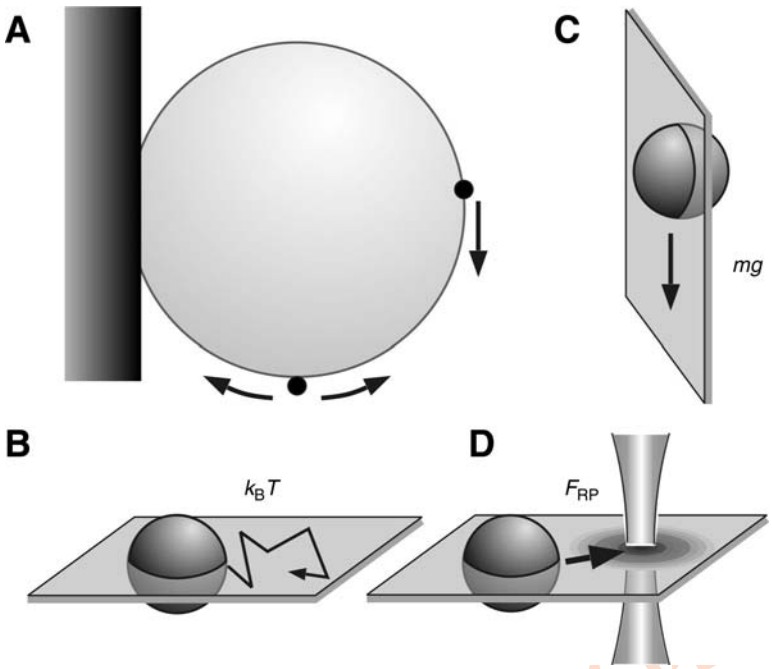

Fig. 2. Three approaches to measure the friction coefficient of a particle moving on a membrane. **(A)** Vesicle fixed to a surface with two possible positions of a particle adhered to the vesicle membrane. **(B)** A Brownian particle experiences a random walk at the bottom (or top) of the vesicle. **(C)** A heavy particle sediments toward the vesicle bottom due to gravity. **(D)** A particle is driven toward the axis of the trap beam because of the radiation pressure force (F_{RP}). The sketch is exaggerated in terms of particle-trap distance.

Note that the surface viscosity has units of (bulk viscosity × length), i.e., dyn.s/cm or surface poises (sp). Using the relation in **Eq. 2** one can estimate the membrane viscosity by measuring the friction coefficient of a small particle attached to the membrane.

Three possible approaches can be used to measure ζ_m (*see* **Fig. 2**). The first is applicable to small Brownian particles of diameter up to about 2 μm **(Fig. 2B)**. Analyzing the trajectory in time of such a particle, one can extract the diffusion coefficient (D), which is inversely proportional to the friction coefficient, according to the Einstein relation. The second approach can be used with larger (heavier) particles attached to the membrane **(Fig. 2C)**. By means of the optical trap the particle is brought to the upper part of the vesicle and released from the trap. Under the influence of its own weight, the particle then starts to sediment following the surface of the vesicle.

Analysis of the sedimentation trajectory gives the friction experienced by the particle. In the third method, the particle motion is driven by the radiation pressure force of the trap (F_{RP}) (*see* **Fig. 2D**). The particle is brought to either the top or the bottom of the vesicle, wherein the membrane is essentially flat and horizontal and the trap is switched on in the direct vicinity of the particle. This results in a sudden motion of the particle center toward the beam axis. Knowing the stiffness of the trap, analysis of the particle trajectory provides the value of the friction coefficient. Finally, the membrane viscosity can be extracted from the friction coefficient using **Eqs. 1** and **2** in all three cases. Performing any of these three procedures at

Job: Dopico
Chapter: 15_Dimova
Template: MIMB/7x10/Temp/01.02.07

Operator: IBH
Date: 17/05/07
Revision: 1st Revises

different temperatures approaching the main phase-transition temperature of the lipid provides the temperature dependence of the membrane viscosity.

1.2. Measuring the Membrane Bending Stiffness Close to the Fluid–Gel Phase Transition

When the temperature is lowered below the main phase-transition temperature of the lipids in the bilayer, the membrane properties change drastically. The fluid-to-gel transition leads to divergence in the shear surface viscosity, whereas the membrane acquires a nonzero shear modulus (in the fluid-state, lipid membranes have zero shear modulus). The membrane elastic properties also change. Lipid membranes in the fluid state are characterized by a bending rigidity in the order of 10 k_BT (exact values for different lipid bilayers can be found in **refs. *8*** and ***9***), where k_B is the Boltzmann constant and T is temperature. When the lipid bilayer undergoes the fluid-to-gel transition, the bending rigidity drops down, and in the gel phase, it increases by a few orders of magnitudes ***(10,11)*** when temperature is decreased. Measuring the bending stiffness of membranes in the fluid state is a handled task, and a large number of methods have already been developed. To mention a few, fluctuation spectroscopy (*see* **ref. *12***) is based on the analysis of membrane undulation of giant vesicle membranes; the micropipet aspiration technique ***(13)*** in the low-tension or entropic regime is based on pulling out membrane fluctuations; analysis of the degree of deformation of giant vesicles subjected to alternating electric fields can also provide the bending stiffness modulus ***(14)***. All these techniques have been applied to lipid membranes in the fluid state. However, in the gel phase the bending stiffness increases dramatically and most of the classical methods cannot be applied. A few new techniques have been recently developed for measuring the bending stiffness of membranes in the gel phase ***(10,11,15)*** and one of them is presented in this article.

When particles are attached to the membrane and the bilayer is brought to the gel phase, the particle motion is hindered (i.e., their motion along the membrane becomes frozen). In a typical experiment, the penetration depth of the particles is usually small, i.e., the contact line with the membrane is far from the equator of the particle, and the particles are located more to the outside of the vesicle (*see* **Fig. 3A**). Two particles (spaced by a few particle diameters) can be manipulated simultaneously using two optical tweezers. The latter are characterized by the trap stiffness, or the trapping constant (k_{RP}). A force (F_{RP}) is applied to displace one of these particles in the membrane plane by a mobile trap while holding the other in the potential well of an immobile or fixed trap. For particle configurations as the one shown in **Fig. 3A**, the main membrane deformation caused by the particle's displacement is bending (*see* **Fig. 3C**). The experiment leads to measuring an apparent membrane spring constant, k_M ***(10)***:

$$k_M = k_{RP}\left[\left(x_m + x_f\right)/\left(l_1 - l_0\right) - 1\right] \tag{3}$$

where x_m and x_f are the displacements of the beads in the mobile and the fixed trap, respectively, and l_0 and l_1 are the distances between the particles before and after applying the forces. The relation between k_M and the membrane bending modulus (κ) is given by an empirical formula ***(10)***:

$$k_M \cong 60\,\kappa/a^2 \tag{4}$$

Job: Dopico
Chapter: 15_Dimova
Template: MIMB/7x10/Temp/01.02.07

Operator: IBH
Date: 17/05/07
Revision: 1st Revises

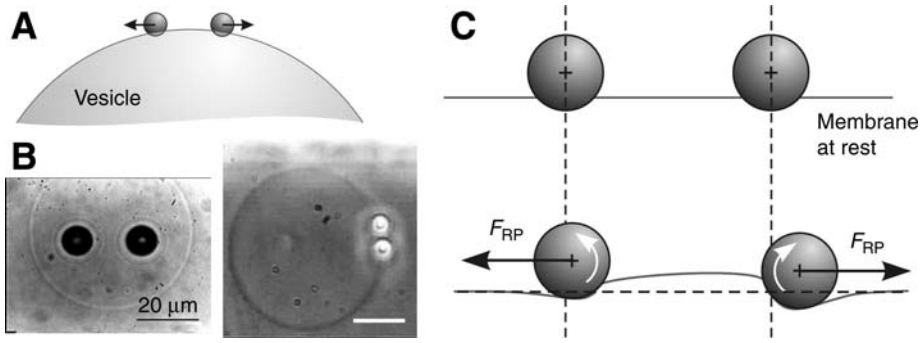

Fig. 3. **(A)** Sketch of two particles adhering to the membrane of a vesicle. **(B) (Left)** Top view (in classical transmission microscopy) of two large particles located on top of a vesicle. The particles are approximately in focus. The image of the vesicle equator, well below the focal plane of the microscope, appears as a clear faint ring. **(Right)** Two smaller particles are located at the vesicle equator. The scene is observed in phase contrast, which provides a dark image of the membrane and bright images of the particles. **(C)** Sketch of the out-of-plane deformation of the membrane (side view) induced by pulling on one of the two particles and keeping the other in the potential well of the fixed trap. The apparent spring constant of the membrane can be calculated by measuring the relative particle displacement.

2. Materials

2.1. Lipids for Vesicle Preparation

Any synthetic phosphatidylcholine can be used as long as the main phase-transition temperature is easily accessible in the laboratory environment. 1,2-dimyristoyl-*sn*-glycero-3-phosphocholine (DMPC) (Avanti Polar Lipids, Alabaster, AL) (no additional purification of the lipid is needed) was used. The DMPC membrane undergoes fluid-to-gel transition around 24°C ***(16)***. The lipid is dissolved in chloroform solution and stored at –20°C. At this temperature, the lipid is stable for up to 3 months.

2.2. Particles for Optical Dynamometry

Both latex (polystyrene) particles and glass beads can be used. In this work mainly latex spheres (Polyscience, Warrington, PA) will be referred to, with diameters ranging from 2 to 12 µm. The particles are stored at 4°C and are stable for a few years. Right before using, a droplet of the particle stock solution is diluted in 2 mL pure water (*see* **Note 1**).

3. Methods

3.1. Vesicle Preparation, Particle Size Determination, and Trap Calibration

The vesicle formation and the particle dynamometry experiments are performed in the same chamber. Giant unilamellar vesicles are prepared following the electroformation method ***(17–19)*** in a chamber with the geometry sketched in **Fig. 4**. During vesicle formation, the temperature was set to 30°C, which is well above the main phase transition of DMPC. The preparation steps are the following:

1. A few droplets of the solution of the lipid dissolved in chloroform at concentration approx 2 mg/mL are deposited on the electrodes (platinum wires of ~1-mm diameter) (*see* **Fig. 4**). The electrodes are left under a nitrogen stream or under vacuum for 2 h, for complete evaporation of the organic solvent.

Job: Dopico
Chapter: 15_Dimova
Template: MIMB/7x10/Temp/01.02.07

Operator: IBH
Date: 17/05/07
Revision: 1st Revises

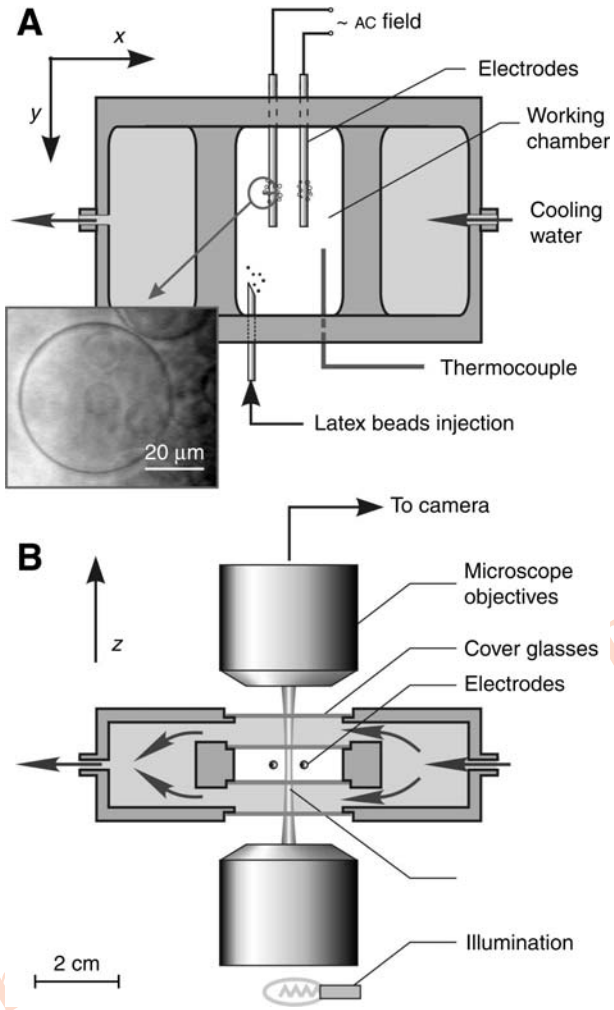

Fig. 4. Sketch of the experimental chamber. **(A)** Top view. **(B)** Side view. Vesicles are grown on both electrodes. The working chamber is surrounded by a cooling water jacket assuring temperature control. A thermocouple measures the current temperature in the working chamber. The top microscope objective (×40, numerical aperture [N.A.] = 0.6) is operated in the phase-contrast mode. The latex particles are injected through a needle (*see* **panel A**). The chamber is mounted on a motorized *x*-*y*-*z* stage.

2. The electrodes are inserted in the chamber. The external compartment (water jacket) is filled with water and a constant flow is assured from a thermostat. The temperature in the chamber is adjusted to 30°C. The electrodes are connected to an AC-field generator and a voltage at 10 Hz and 0.3 V/mm is supplied for 10 min. The working chamber is slowly filled with water (*see* **Note 2**), which is introduced through a needle (the same needle is later used for introducing the latex particles).
3. After the first 20 min the voltage in the chamber is gradually increased to about 1.2 V/mm in 0.3 V/mm steps every 20 min and the sample is left at these field conditions for another couple of hours. The vesicles can be found along the electrodes. The procedure is terminated by slowly decreasing the voltage to 0.5 V/mm and the frequency changed to 5 Hz for about 5 min, which helps detaching the vesicles from the electrode. The vesicles near the outer boundary of the clusters formed at the electrodes (*see* snapshot in **Fig. 4A**) are most convenient for working (*see* **Note 3**).

Job: Dopico
Chapter: 15_Dimova
Template: MIMB/7x10/Temp/01.02.07

Operator: IBH
Date: 17/05/07
Revision: 1st Revises

4. A few tens of microliter of the latex bead solution are introduced in the working chamber (a microliter syringe is used). A particle is captured "in flight" by the laser beam at the exit of the syringe needle (*see* **Note 4**).
5. Particle size (a) measurement: if the particle is small, a is determined from the diffusion path of the particle in water (D_{free}). Conversely, the size of a heavy particle is deduced from its sedimentation velocity (v_{sed}). In the former case, the bead radius is given by the Stokes–Einstein relation $a = k_B T / 6\pi\eta D_{free}$ (*see* **Note 5**). In the latter case, the application of Stokes' law gives $a = (9\eta v_{sed} / 2\Delta\rho g)^{1/2}$, where $\Delta\rho$ is the density difference between water and polystyrene ($\approx 0.05 g/cm^3$) and g is the gravity acceleration (*see* **Note 6**).
6. To calibrate the radiation pressure force (F_{RP}), the trapped sphere is submitted to a constant counter-flow of known velocity (this is done by moving the stage on which the chamber is mounted with a fixed velocity). The "escape" velocity (v_{esc}) at which the particle leaves the trap is determined. The corresponding trapping force, which is the maximum of F_{RP}, balances the viscous drag force (Stokes' law): $F_{RP} \cong 6\pi a\eta v_{esc}$. The trap spring constant is given by $K_{RP} \cong 6\pi\eta v_{esc}$.
7. Finally, the particle is brought in contact to a selected vesicle. In this procedure, the particle is held fixed in space, while the whole chamber is moved by motorized stages. When in contact with the vesicle, the particle spontaneously adheres to the membrane. Once completed, adhesion is irreversible: it is not possible to detach the particle applying radiation pressure forces (several tens of pN).

3.2. Shear Surface Viscosity Measurements

The procedure involves measuring ζ at different temperatures, and deducing η_S at each step. It starts at $T = 30°C$, and proceeds through successive temperature steps. After each step, the sample is left at rest until thermal equilibrium is reached (this takes about 15 min). At temperatures $\leq 22°C$, the shear viscosity of DMPC membranes is so high that motion of the latex beads is no longer optically detectable. An example of data obtained from the three procedures applied to the same vesicle-particle system is given in **Fig. 5**.

3.2.1. Brownian Motion Dynamics

1. A small particle (radius <2 μm) adhering to the vesicle membrane is brought to the bottom or top of the vesicle and the trap is switched off (*see* **Fig. 2B**).
2. The particle trajectory is recorded for a period of time enough to collect about 400 data points (when the lipid bilayer is in the fluid phase, 100 s of recording at acquisition frequency of approx 6 Hz suffices; however, at temperatures approaching the gel phase longer acquisition times are necessary).
3. The mean square displacement of the particle is determined and the diffusion coefficient extracted:

$$\left\langle (\Delta x)^2 + (\Delta y)^2 \right\rangle = 4D\Delta t \tag{5}$$

   where t is time.

4. The friction coefficient is then determined from the Stokes–Einstein relation, $\zeta = k_B T / D$.

3.2.2. Sedimentation Velocity Measurements

1. A large or heavy particle (for latex particles the size should be above 3 μm in radius) adhered to the vesicle membrane is brought to the top of the vesicle and the trap is switched off (*see* **Fig. 2C**).
2. The trajectory over time of the particle sedimenting toward the vesicle bottom is recorded. As the observation is from above the moving particle quickly gets out of focus, leading to frequent

Job: Dopico
Chapter: 15_Dimova
Template: MIMB/7x10/Temp/01.02.07

Operator: IBH
Date: 17/05/07
Revision: 1st Revises

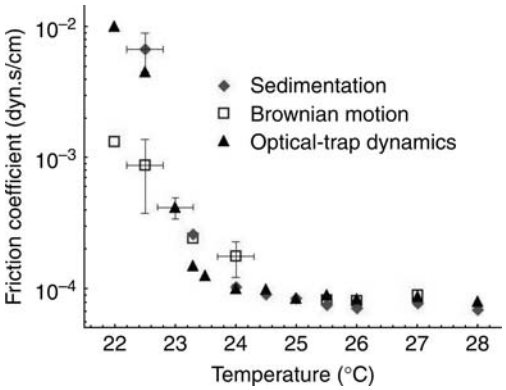

Fig. 5. Examples of data collected using the three described procedures with the same vesicle-particle system. The particle size is $a = 3.2$ μm, and the vesicle size is 21 μm.

refocusing. The coordinates of the vesicle center are determined from a snapshot taken in the equatorial plane.

3. The distance between the particle and vesicle centers, $r(t)$, is extracted from the recorded particle trajectory. It is described by the equation (7):

$$r(t) = r_{max}\sin\left\{2\arctan[\exp(4\pi a^3\Delta\rho g t/3\zeta r_{max})]\tan(\theta_0/2)\right\} \quad (6)$$

where the angle θ_0 is defined by $\sin\theta_0 = r(t=0)/r_{max}$.

This equation is used to fit the experimental curve and to extract the bead friction coefficient.

3.2.3. Optical Trapping Dynamics

1. A particle of several micrometers in radius is brought to the top or the bottom of the vesicle and the trap is switched off. The experimental chamber is displaced in the horizontal plane by a distance approx $0.6a$. The trap is then switched on, and the trajectory of the particle toward the beam axis is recorded over time (*see* **Fig. 2D**).
2. The time dependence of the distance $d(t)$ between the particle center and the trap axis is extracted from the particle trajectory. The data is fitted to by $d(t) = d(t=0)\exp(-tk_{RP}/\zeta)$, providing the particle friction coefficient.

3.3. Measuring the Membrane Bending Stiffness Close to the Fluid–Gel Phase Transition

1. Two particles of similar size and several microns in radius are brought to the top or the bottom of the vesicle by means of the double optical trap. It is a requirement that both penetration depths of the particles are small (*see* **Fig. 3C**). This condition is in general fulfilled when more than one particle are brought to adhere to the vesicle membrane.
2. The temperature of the chamber is lowered to 15°C, and the sample is let to equilibrate.
3. The initial distance between the traps (l_0) is measured, and the location of the particles centers is determined. The mobile trap is shifted by approx $0.6a$ in direction away from its initial position, away from the fixed trap. The new intertrap distance (l_1) is measured, as well as the relative displacements of the particle in the mobile trap (x_m) and the particle in the fixed trap (x_f).
4. The membrane spring constant (k_M) is determined using **Eq. 3**. The bending stiffness of the membrane is deduced from **Eq. 4**.

5. The temperature is increased by a few degrees, and **steps 3** and **4** are repeated. Thus, the temperature dependence of the membrane bending stiffness is obtained when the lipid bilayer approaches its gel-to-fluid phase transition. The work is completed when $T = 24°C$, and the membrane is in the fluid state.

4. Notes

1. Unless stated otherwise, all solutions should be prepared in water that has a resistivity of 18.2 MΩ.cm. This standard is referred to as "water" in this text.
2. The water used to fill the working chamber should be degassed before introducing it in the chamber. This prevents the formation of bubbles during work.
3. At the end of the electroformation procedure, the vesicles are usually interconnected and clustered. Target vesicles are selected at the outer rim of such clusters for experiments wherein vesicles that are unilamellar (as far as one can determine from phase contrast views) and without obvious internal structures are easily found.
4. It is important to trap a particle "in flight" at the exit of the syringe needle. One might be tempted to simply catch one of the many particles that have been released and lie on the floor of the chamber. Experience shows that such particles often do not adhere on the vesicle membranes. The reason for this is unclear; it is supposed that the surfaces of the particles, when hitting the walls of the chamber, get contaminated by traces of lipids. Apparently (and fortunately) the bulk water inside the chamber is free from lipids.
5. When the temperature in the chamber is changed, the bulk water viscosity changes; this has to be taken into account when performing the calculations for the particle radius and the friction coefficient; *see* **Eq. 2**.
6. The density difference between latex (or particle material) and water can be measured independently in the following way: the particles are diluted in solutions of glycerol of various densities (i.e., various concentrations of glycerol in water). The solutions are centrifuged. The density at which the particles neither sediment to the bottom of the centrifuge tube nor cream to the surface of the solution is corresponding to the particle material density.

References

1. Ashkin, A. (1970) Acceleration and trapping of particles by radiation pressure. *Phys. Rev. Lett*. **24,** 156–159.
2. Angelova, M. I. and Pouligny, B. (1993) Trapping and levitation of a dielectric sphere with off-centered Gaussian beams. I. Experimental. *Pure Appl. Opt. A* **2,** 261–276.
3. Dietrich, C., Angelova, M. I., and Pouligny, B. (1997) Adhesion of latex spheres to giant phospholipid vesicles: statics and dynamics. *J. Phys. II France* **7,** 1651–1682.
4. Dimova, R., Dietrich, C. and Pouligny, B. Motion of particles attached to giant vesicles: falling ball viscosimetry and elasticity measurements on lipid membranes, in Giant Vesicles, ed. Luisi, P. L., and Walde, P. (1999) John Wiley and Sons, New York, pp. 221–230.
5. Danov, K. D., Dimova, R., and Pouligny, B. (2000) Viscous drag of a solid sphere straddling a spherical or flat surface. *Phys. Fluids* **12,** 2711–2722.
6. Dimova, R., Danov, K., Pouligny, B., and Ivanov, I. B. (2000) Lateral motion of a large solid particle trapped in a thin liquid film. *J. Coll. Interface Sci.* **226,** 35–43.
7. Dimova, R., Dietrich, C., Hadjiisky, A., Danov K., and Pouligny, B. (1999) Falling ball viscosimetry of giant vesicle membranes: finite-size effects. *Eur. Phys. J. B* **12,** 589–598.
8. Seifert, U. and Lipowsky, R. (1995) Morphology of vesicles. in *Structure and Dynamics of Membranes*, (Lipowsky, R. and Sackmann, E., eds.), Elsevier, Amsterdam, pp. 403–463.
9. Rawicz, W., Olbrich, K. C., McIntosh, T., Needham, D., and Evans, E. (2000) Effect of chain length and unsaturation on elasticity of lipid bilayers. *Biophys. J*. **79,** 328–339.
10. Dimova, R., Pouligny, B., and Dietrich, C. (2000) Pretransitional effects in dimyristoylphosphatidylcholine vesicle membranes: Optical dynamometry study. *Biophys. J.* **79,** 340–356.

11. Mecke, K. R., Charitat, T., and Graner, F. (2003) Fluctuating lipid bilayer in an arbitrary potential: theory and experimental determination of bending rigidity. *Langmuir* **19,** 2080–2087.
12. Méléard, P., Gerbaud, C., Pott, T., et al. (1997) Bending elasticities of model membranes—influences of temperature and sterol content. *Biophys. J*. **72,** 2616–2629.
13. Evans, E. and Rawicz, W. (1990) Entropy-driven tension and bending elasticity in condensed-fluid membranes. *Phys. Rev. Lett*. **17,** 2094–2097.
14. Kummrow, M. and Helfrich, W. (1991) Deformation of giant lipid vesicles by electric fields. *Phys. Rev. A* **44,** 8356–8360.
15. Lee, C. -H., Lin, W. -C., and Wang, J. (2001) All-optical measurements of the bending rigidity of lipid-vesicle membranes across structural phase transitions. *Phys. Rev. E* **64,** 020901.
16. Koynova, R. and Caffrey, M. (1998) Phases and phase transitions of the phosphatidylcholines. *Biochim. Biophys. Acta* **1376,** 91–145.
17. Angelova, M. I. and Dimitrov, D. S. (1986) Liposome electroformation. *Faraday Discuss. Chem. Soc.* **81,** 303–311.
18. Angelova, M. I., Soléau, S., Méléard, P., Faucon, J. F., and Bothorel, P. (1992) Preparation of giant vesicles by external AC electric fields. Kinetics and applications. *Prog. Colloid Polym.* **89,** 127–131.
19. Dimova, R., Aranda, S., Bezlyepkina, N., Nikolov, V., Riske, K. A. and Lipowsky, R. (2006) A practical guide to giant vesicles. Probing the membrane nanoregime via optical microscopy. *J. Phys. Condens. Matter* **18,** S1151–S1176.